MR. GUSTAV SEIXAS (Orcid ID : 0000-0002-3361-8064)

Article type   : Technical Paper

Historical and Future Stream Temperature Change Predicted by a Lidar-Based Assessment of Riparian Condition and Channel Width

Gustav B. Seixas, Timothy J. Beechie, Caleb Fogel, and Peter M. Kiffney

Ocean Associates Inc. (**Seixas**, **Fogel**), under contract to National Marine Fisheries Service, Arlington, Virginia, USA; and Northwest Fisheries Science Center, (**Beechie**, **Kiffney**), National Oceanic and Atmospheric Administration, Seattle, Washington, USA (Correspondence to Seixas: gseixas@skagitcoop.org).

Abstract: Riparian forests attenuate solar radiation, thereby mediating an important component of the thermal budget of streams. Here, we investigate the relationship between riparian degradation, stream temperature and channel width in the Chehalis River basin, WA State, USA. We used lidar data to measure canopy opening angle, the angle formed between the channel center and trees on both banks; we assumed historical tree heights and calculated the change in canopy angle relative to historical conditions. Next, we developed an empirical relationship between canopy angle and water temperature using existing data, and simulated temperatures between 2002 and 2080 by combining a tree growth model with climate change scenarios from the NorWeST regional prediction. The greatest change between historical and current conditions (~7 ˚C) occurred in developed portions of the river network, with the highest values of change predicted at channel widths <~40 m. Tree growth lessened climate change increases in maximum temperature and the length of river exceeding biologically-critical thresholds by ~50-60 %. Moreover, the maximum temperature of channels with bankfull widths <~50 m remained similar to current conditions despite climate change increases. Our findings are consistent with a possible role for the riparian landscape in explaining the low sensitivity of stream temperatures to air temperatures observed in some small mountain streams.

(**Key Terms:** Riparian; stream water temperature modeling; lidar; salmon; Chehalis River; river restoration.)

Introduction

Riparian forest structure controls the amount and quality of light reaching stream surfaces, in turn influencing habitat suitability and connectivity, primary production, and water quality (Brosofske, Chen et al. 1997; Kiffney, Richardson et al. 2003; Kaylor, Warren et al. 2017). Incoming solar radiation is one of the most important factors controlling stream temperature (Brown and Krygier 1970; Beschta 1997; Poole and Berman 2001), a master variable in aquatic ecosystems affecting rates of decomposition, nutrient cycling, and individual growth of aquatic organisms. Solar input is therefore a critical parameter influencing habitat in cold water systems that support ecologically and economically important species such as salmon, trout and charr (Beschta, Bilby et al. 1987; Hicks, Hall et al. 1991). Despite their critical function, riparian forests have been altered extensively in many temperate river basins (e.g. Macfarlane, Gilbert et al. 2016), fueling the need for watershed-scale analyses that identify locations where restoration efforts have the highest potential for affecting change.

The need to understand spatial patterns of stream temperature is especially important in watersheds containing Pacific salmon (*Oncorhynchus* spp.), which are listed under the Endangered Species Act and have upper lethal temperature limits ranging from 23.8 to 25.1 ˚C (Brett 1952; McCullough, Spalding et al. 2001). Stream water temperatures to which salmon and other cold water species have locally adapted are controlled by a complicated set of physical interactions between the air-water and the channel bed-water interfaces (Brown 1972; Beschta 1997; Poole and Berman 2001; Moore, Spittlehouse et al. 2005), as well as physiographical (slope, discharge, elevation) climatological (precipitation), and hydrological (rain-dominated vs. snow-dominated hydrograph) effects. The physical processes controlling water temperature are further complicated in streams due to turbulence, tributary confluence inputs, and systematically-varying longitudinal effects such as increasing flow volume with distance from the source of overland flow (Vannote, Minshall et al. 1980; Kiffney, Greene et al. 2006; Fullerton, Torgersen et al. 2015). An additional complication is that the relationship between temperature and biological processes is non-linear—for example, effects on salmonid growth and survival may be negative above threshold water temperatures because metabolic costs exceed gains (Armour 1991; McCullough, Spalding et al. 2001).

Despite the complications posed by the myriad influences on stream temperature, it has been well-documented in the literature that reduction or removal of riparian shade results in significant warming. Amongst 18 studies that employed a rigorous before-after effect size study design, Moore, Spittlehouse et al. (2005) found a median after-treatment warming of 2.5 ˚C, while the maximum warming was 11.6 ˚C. The large range likely reflects different discharges and water depths at which the measurements were taken, differences in the hydrology of the study basins, differences in air temperature and elevation between basins and between years, varying basin aspects, and varying degrees of canopy removal. However, the overall pattern is clear: reduction in riparian shade leads to quantifiable, if highly variable, increases in summertime maximum stream temperatures that may render portions of the stream network energetically unprofitable or even uninhabitable to salmonids.

Because high water temperature is a critical management concern for a variety of species, a number of empirical and process-based models exist for predicting stream temperature at the scale of reaches (e.g. Brown 1972; Beschta and Weatherred 1984), river basins or regions (e.g. Chen, Carsel et al. 1998; Boyd and Kasper 2003; Allen, Dietrich et al. 2007; Isaak, Wenger et al. 2011) and continents (Hill, Hawkins et al. 2013). However, the reach-scale models require data that may be difficult or impossible to collect across an entire watershed; conversely, basin-, regional-, and continental-scale models may miss critical spatial variation in individual watersheds due to the coarseness of input data. Moreover, empirical models typically relate stream temperature to basin and climatological data aggregated from point locations across many basins (Isaak, Wenger et al. 2011; Hill, Hawkins et al. 2013); this approach has the benefit of capturing physical variables known to influence stream temperature, yet fails to directly measure riparian condition variability within individual basins. Consequently, it has been difficult to quantify potential benefits of shade restoration across a large watershed and to accurately identify sites with the greatest potential for reducing stream temperatures.

Because natural channels widen with increasing drainage area (Leopold and Maddock 1953; Montgomery and Gran 2001), the impact of shade reduction on stream temperature is expected to vary spatially throughout watersheds. For example, high-order, wide channels are exposed to high levels of solar radiation under natural conditions (Davies-Colley and Quinn 1998); therefore, these channels may not experience much change in temperature when riparian forests are removed or altered. In contrast, mid-order tributaries should undergo larger changes in temperature if riparian shade is reduced, while low-order tributaries with widths less than 3.5 m may be relatively insensitive to reduction in riparian forest height because even small shrubs will shield much of the water surface for at least portions of the day (Fig. 1) (Davies-Colley and Quinn 1998). Because riparian zones in many temperate watersheds have been subject to management for many decades, the above relationships suggest the likelihood that there is a patchwork of temperature quality along the length of river networks that is dependent on position in the network and degree of riparian alteration.

Moreover, climate change is expected to increase summertime maximum stream temperatures and to expand portions of river networks that exceed biologically-critical temperature thresholds (Isaak, Wollrab et al. 2012; Hill, Hawkins et al. 2014; Isaak, Young et al. 2016). While the sensitivity of stream temperature to climate change is known to depend on geomorphology and hydrology (Luce, Staab et al. 2014; Lisi, Schindler et al. 2015), the role of riparian shade in moderating the effects of climate change on stream temperatures has not been addressed within a basin scale spatial context. Thus, one outstanding question is whether restoring riparian shade in different positions of the river network will differentially mitigate climate change effects on stream temperature due to the hydraulic geometrical effects mentioned above.

Figure 1.

In this paper we investigate the hypothesis that maximum potential stream temperature increases due to riparian vegetation reduction—and therefore the greatest potential for shade restoration—occur at intermediate and small channel widths (Figs. 1, S1). An extension of this hypothesis is that geomorphic processes, through their control of hydraulic geometry, dictate the spatial locations on the landscape where riparian restoration will have the most impact on stream temperature. We used lidar data (a form of high-resolution remotely-sensed data that captures tree heights) to calculate the current canopy opening angle, which accounts for the tradeoff between tree height and channel width in dictating riparian shade, throughout the Chehalis River basin in southwestern Washington State, USA. Next, we developed an empirical water temperature model using existing data. These techniques allowed us to combine the advantages of high-resolution remotely-sensed data and broad spatial coverage to model the relationship between stream shade and water temperature across a large river basin. We then used estimated mature tree heights from known species distributions to inform a reference condition of historical (pre-European-American settlement and widespread logging) stream temperatures and to calculate change in canopy opening angle and water temperature as two measures of riparian degradation. Finally, we modeled future stream temperature changes due to tree growth and climate change by applying an empirical tree growth model and the climate change increases from the NorWeST regional database (Isaak, Wenger et al. 2011) to our riparian inventory. The predictions of future water temperature allowed us to assess spatial and temporal patterns of stream temperature change between the current condition and 2080.

Study Location

The Chehalis River is located in southwestern Washington State, USA (Fig. 2). The river's drainage area, which exceeds 5,500 km^2 at its delta in Grays Harbor, is distributed across pristine upland regions in Olympic National Park, lowland urban and agriculture areas, and active timber lands in the Olympic Mountains, Willapa Hills, and Cascade foothills. Maximum annual precipitation can exceed 6,000 mm in the Olympic mountains but more typical values are in the 1,000-2,000 mm range (PRISM Climate Group 2012).

Figure 2.

The basin lies within the Pacific Coastal Forest region extending from northern California to Alaska. Dominant deciduous broadleaf species include willow (*Salix spp.*), red alder (*Alnus rubra*), Black cottonwood (*Populus trichocarpa*), and big leaf maple (*Acer macrophyllum*), while dominant coniferous species include Douglas-fir (*Pseudotsuga menziesii*), Sitka spruce (*Picea sitchensis*), western hemlock (*Tsuga heterophylla*), and western red cedar (*Thuja plicata*) (Franklin and Dyrness 1973). The general successional pattern is from hardwood to conifer, with young patches occupied by colonizing species such as willow, alder and cottonwood, and old patches occupied by late successional species such as Douglas-fir, Sitka spruce, western hemlock, and western red cedar (Crocker and Major 1955; Fonda 1974).

Seven species of anadromous salmonids use the Chehalis River and its tributaries: Chinook salmon (*Oncorhynchus tshawytscha*), coho salmon (*O. kisutch*), chum salmon (*O. keta*), pink salmon (*O. gorbuscha*), steelhead (*O. mykiss*), cutthroat trout (O. clarkii), and Bull trout (Salvelinus confluentus) (Sandell, Fletcher et al. 2014). Because Chinook, coho, and steelhead, along with non-migratory fishes, utilize freshwater habitats during the month of August when water temperatures typically reach their maximum, these species are the most affected by shade reduction.

Methods

Reference condition for riparian analysis

To define riparian reference conditions (i.e. the natural potential tree height), we first stratified the basin into floodplain channels with varying rates of lateral channel migration and floodplain turnover, and non-floodplain channels with stable riparian landforms (small terraces or hillslopes). We used a threshold of 20 m bankfull width—defined as the width at water flows that fill the active channel but before spillage onto the floodplain (Leopold, Wolman et al. 1964)—to distinguish between floodplain and non-floodplain channels. We used this threshold because Beechie, Liermann et al. (2006) found that western Washington channels narrower than 20 m had a stable planform geometry and were able to develop stands of late-successional conifer trees. Channels wider than 20 m were subject to more frequent disturbance by lateral migration or avulsion and thus were characterized by a mix of early and late successional species of both deciduous and conifer trees (Naiman, Bechtold et al. 2010). We describe our process for calculating bankfull width below.

Floodplain channels erode their floodplains with average return intervals ranging from 8 to 89 years, depending on channel pattern (Beechie, Liermann et al. 2006). This creates many small stands of varying ages and species compositions dominated by early successional species such as willow, red alder, and Black cottonwood (Agee 1988; Van Pelt, O'Keefe et al. 2006) (Fig. S2). Non-floodplain channels have floodplain widths commonly less than 4 times the active channel width and are typically dominated by conifers in western Washington (Beechie, Pess et al. 2000; Rot, Naiman et al. 2000; Beechie, Liermann et al. 2006) (Fig. S2). Non-floodplain riparian areas in the Chehalis River basin are in the western hemlock or Sitka spruce zone (Franklin and Dyrness 1973), which have fire return intervals between 180 and 230 years (Agee 1993). The principle successional pathway is characterized by Douglas-fir colonization and dominance during the first 200-300 years after fire, followed by succession to western hemlock or Sitka spruce as the stand ages beyond 300 years (Munger 1940; Franklin and Dyrness 1973).

Therefore, for the historical condition along non-floodplain channels we assumed mature dense conifer stands with a site potential tree height of 52 m. This height is based on growth trajectories in (McArdle, Meyer et al. 1930), descriptions found in Gannett (1899), and the average tree height at six present-day old-growth sites in the Stillaguamish River basin (48 m; M. Pollock, unpublished data). For mixed forests along floodplain channels, we used a typical tree height for mature hardwoods of 30.5 m. The value is meant to represent an approximate weighted average of red alder (~30 m), Black cottonwood (~40 m), and willow (~6 m). For comparison, the weighted average height of species found on Stillaguamish River floodplains was 29 m and 34 m for the mainstem and North Fork, respectively (M. Pollock, unpublished data).

Data

Our analysis relied primarily on airborne lidar data compiled by the Puget Sound lidar Consortium (Fig. 2). Light Detection and Ranging (lidar) data has been shown to be effective for forest ecological applications due to its ability to measure the elevation of the ground surface as well as tree heights over large regions at high resolution (e.g. Means, Acker et al. 2000; Seavy, Viers et al. 2009). The lidar datasets curated by the PSLC come from multiple sources, yet most of the acquisitions used here had an original spatial resolution of approximately 3 feet. During the processing steps (below) we sampled the DEMs to conform to exactly 1 m spatial resolution in our chosen UTM projection. Positional accuracy of the datasets, where reported on the PSLC website, varied from 0.084 ft to 0.21 ft (RMSE calculated using a network of real time kinematic GPS ground control points). We used a Python script and ArcGIS geoprocessing tools to pre-process the bare earth and 'first-returns' DEMs, including projection, pit filling, flow direction calculation, and creation of ASCII text files. Next, we read the text files into Matlab using the function ReadArcGrid.m (T. Perron, http://web.mit.edu/perron/www/downloads.html) and created maps of the forest canopy by subtracting the un-filled bare earth DEM from the first return data (Fig. 2).

We modeled bankfull channel width for the entire channel network by multiple linear regression using contributing drainage area and upstream mean precipitation as predictor variables (Sumioka, Kresch et al. 1998; Davies, Lagueux et al. 2007). We calculated contributing area using the D8 flow accumulation of a 10 m resolution DEM from the National Elevation Dataset. For the precipitation data, we used the most recent (1981-2010) 30 year normal PRISM precipitation grid (PRISM Climate Group 2012), subsampled to 10 m resolution to match the DEM.

Starting with a GIS file of Chehalis River basin channel reaches from the National Hydrography dataset (U.S.G.S 2013), we extracted contributing area directly from the flow accumulation grid to the midpoint of each reach. Next, using ArcGIS geoprocessing tools and a Python script, we delineated the entire watershed upstream of each reach, clipped the precipitation data to the watershed, found the mean value of the clipped precipitation grid, and assigned that value to the reach. We measured bankfull channel width at 106 locations throughout the basin by hand in ArcMap, using aerial photography and hillshade images of the lidar DEMs to distinguish channel banks. At each location, we extracted contributing area and upstream mean precipitation using the method described above. With these data we constructed a linear model that predicts channel width as a function of contributing area and upstream mean precipitation. We found that the model fit was aided by stratifying the data into two groupings, one group for tributaries draining the Olympic Mountains (R^2 = 0.59) and one group for all other tributaries and the mainstem (R^2 = 0.74). The scatter represents error associated with PRISM data, the DEM used to calculate flow accumulation, and remote measurement of bankfull width, as well as natural variation.

Canopy opening angle change

Canopy opening angle is the angle formed between the stream thalweg (i.e. line of highest accumulated flow along a stream system) at the water surface and the top of the first shade-providing tree on either bank (Fig. 1). Rutherford, Blackett et al. (1997) used a similar metric as input for a computer model that predicted water temperature from vegetative and topographic shading. We extend this concept by focusing on change to the canopy opening angle due to disturbance (i.e. removal of shade) and regrowth (Fig. S1). The reason for focusing on canopy opening angle change, and not current canopy opening angle, is that our goal is to help focus riparian restoration on areas that have undergone large canopy changes and that have the most potential for returning to natural conditions.

Canopy opening angle, θ [˚], and canopy opening angle change, Δθ [˚], are calculated by

$$\theta_{c,h} = \left(90 - \mathrm{atan}\left(\frac{H_1}{W_1}\right)\right) + \left(90 - \mathrm{atan}\left(\frac{H_2}{W_2}\right)\right) \tag{1a}$$

$$\Delta\theta = \theta_c - \theta_h \tag{1b}$$

where H_1 and H_2 are tree height plus bank height on each side of the channel, W_1 and W_2 are the horizontal distances from the thalweg to the first tree, θ_c is the current canopy opening angle and θ_h is the historical canopy opening angle. The inverse tangent functions are subtracted from 90˚ such that a channel with complete canopy closure will have θ = 0˚ and a channel with no vegetation or bank topography on either side will have θ = 180˚. In our analysis, the thalweg location is calculated directly from the flow direction raster, i.e. thalweg pixels are those found to be along the path of highest flow accumulation by the bare earth lidar DEMs. In other words, the thalweg is a feature of the digital representation of the landscape; it is not imposed by some additional source of data. While lidar data are highly accurate, in reaches of very low slope and/or very wide water surfaces, the flow direction algorithm may produce thalwegs that deviate from the center of the channel. Wide, low slope channels are predicted to be locations where riparian condition has the least effect on stream temperature; therefore, we expect this source of error to not greatly affect the results.

We manually selected coordinates to begin data collection in ArcMap by digitizing points within the main channels near their upstream termini (hereafter these points are referred to as channel heads). Next, we used an algorithm developed in Matlab to measure riparian condition at specified intervals along the channels flowing from each channel head (a version of the code is available on the lead author's github page; see Data Availability statement). Briefly, the algorithm iterates through each channel head within each DEM tile and searches down the flow direction pathway finding all channel thalweg cells; next, the algorithm extracts thalweg cells at the transect spacing interval (10 m in this study), finds the angle perpendicular to the channel by bisecting the angles formed between the current channel cell and upstream and downstream points, and projects a channel-perpendicular transect 100 m to each side of the channel using the Bresenham line algorithm (Bresenham 1965). Then, the algorithm extracts H_1, H_2, W_1 and W_2 by finding the first cell along the transect (in both directions) that exceeds a height threshold and uses these values to calculate the current canopy opening angle (eq. 1). Because we focus on stream temperatures during the month of August, when the sun is high in the sky for much of the day in the Pacific Northwest, we expect bank topography to play a larger role in shading stream surfaces than far field topographic features. Therefore topographic shading is incorporated at this step by differencing the bare earth elevation of the transect center point from that of the shade-forming vegetation cell, and adding this value to the total tree height. If no vegetation is found, the canopy opening angle is calculated using topography alone. We made no attempt to incorporate topographic shading by features farther from the channel than the transect length (100 m).

During troubleshooting we discovered that in some cases the transect cell closest to the thalweg that exceeded the tree height threshold was in fact a short tree, and a taller tree lay directly behind the cell that was chosen by the algorithm. In these cases, the first point chosen was 'shielding' the taller tree behind, causing an underestimation of shade at that point. To correct this, we used an iterative process in which the algorithm uses a range of height threshold values (we used thresholds of 5, 10, 20, 30, 40, 50, 60, 70, 80, 90 m to test a wide range), and extracts the W and H that minimize the canopy opening angle. The algorithm then extracts the modeled bankfull width at the transect from the nearest NHD stream reach segment. If the bankfull width is larger than 20 m, a reference height of 30.5 m is used, along with W_1 and W_2, to calculate the historical canopy opening angle (see reference condition section, above). If the bankfull width is narrower than 20 m, 52 m is used as the historical height. Canopy opening angle change (Δθ) is the current canopy opening angle θ_c minus the historical canopy opening angle (θ_H) (eq. 1).

Where there is no vegetation present, the canopy opening angle is equal to 180˚. However, the canopy opening width for the historical condition is undefined because the algorithm cannot recognize channel edges and thus W_1 and W_2 are undefined. Thus, for transects in which no vegetation was found under the current conditions, we used the modeled bankfull width as a surrogate for $W_1 + W_2$ in equation 1 under the assumption that bankfull width is similar to the historical canopy opening width under natural conditions.

Empirical relationship between canopy angle and stream temperature

Due to the complicated hydrological, physiographical, and climatological variables that control stream temperature, it is difficult to construct a rigorous model of water temperature that is accurate at the high spatial resolution of our riparian dataset. Our goal was to develop a conceptually-simple model that is able to predict current and future water temperature under a range of riparian restoration scenarios, while acknowledging the uncertainty introduced by the inherent variability in stream temperature data. To construct the model, we used the maximum weekly mean temperature (MWMT) for the month of August (typically the most critical time period for cold water fishes in this region) in the NorWeST stream temperature database (Isaak, Wenger et al. 2011) that lie within the Chehalis River basin. There are eleven unique data locations in the mainstem Chehalis River and some of the major tributaries (Fig. 2A). At most locations, multiple years of data are represented. We treated each year at each location as a separate data point; there are a total of 57 unique year-location entries. The eleven unique locations are distributed throughout the basin with three sites in the mainstem, one site in the South Fork Chehalis River, one site in the East Fork Satsop River, one site in the West Fork Satsop River, two sites in the East Fork Humptulips River and two sites in the West Fork Humptulips River (Fig. 2A).

The distance over which flowing water equilibrates to its surroundings increases with increasing stream size (due to increased water volume and greater thermal inertia), and may also vary due to the riparian condition of the reaches through which it flows (Sullivan, Tooley et al. 1990; Moore, Spittlehouse et al. 2005; Caissie 2006). Values reported in the literature for the equilibration length scale are commonly in the range of 150 to 200 m for small streams (Zwieniecki and Newton 1999; Story, Moore et al. 2003). However, Rutherford, Blackett et al. (1997) presented modeling results suggesting that first order streams could equilibrate ~85 % faster than third order streams to a downstream 50 % reduction in riparian cover. Given this uncertainty, we chose to use the mean value of canopy opening angle within 300 m upstream of each NorWeST data point. This 300 m length encompasses the commonly-published values but also reflects the longer recovery distance in larger channels.

Water temperature is also a function of drainage area, slope, and elevation, among other factors, which do not change over the timescale of riparian degradation or restoration. To capture these effects, we appended contributing drainage area to each NorWeST temperature location and used the logarithm of area as a predictor in the model. Because drainage area and canopy opening angle are correlated in most drainage basins due to channel widening, we conducted two model runs, one using drainage area as the lone predictor and one with drainage area along with canopy opening angle.

Most NorWeST site locations within the Chehalis River basin contain data for multiple years (there are 18 unique years represented in the dataset, 1993-1998, 2001-2012). To test for possible bias by year we ran a cross validation test in which we systematically removed each year represented in the data and ran a multiple linear regression on the remaining data before reinstating the selected year and re-running the analysis. The goal was to assess whether individual years biased the mean result.

The minimum drainage area in the NorWeST database is 14.8 km^2, while the minimum drainage area in the riparian database is 0.0012 km^2. The model tended to underestimate temperature at drainage areas lower than ~15 km^2 due to lack of predictor data at these low drainage areas; therefore, we truncated the temperature model results at the minimum temperature predicted by the model at the NorWeST data locations (13.4˚C).

Future predictions of stream temperature with climate change and tree growth

Our prediction of future water temperature combined the effects of a tree growth model and climate change. We used data in McArdle, Meyer et al. (1930) and Harrington and Curtis (1986) to find tree growth functions (height as a function of age) for Douglas-fir and red alder, which we fit with models of the form ax/(b+x) using an iterative least squares estimation technique. We used the Douglas-fir model to represent conifer growth along non-floodplain channels. Western hemlock and Sitka spruce, the other dominant conifer species in the field area, have similar growth trajectories to Douglas fir (Farr 1984; Beechie, Pess et al. 2000). We used the red alder model to represent growth of predominantly deciduous forests along floodplain channels. Red alder attains maximum heights that are between willow and Black cottonwood, and therefore best approximates the growth rate and mean height of floodplain forests (see reference condition section above). We inverted these models to compute the current age of the trees on both banks at each riparian transect location based on current height.

To incorporate the effects of climate change, we applied predicted water temperature increases from the NorWeST stream temperature model to our riparian dataset locations. The NorWeST model includes predictions based on global average changes to air temperature and stream flow in the 2040's and 2080's following the A1B climate change scenario (Isaak, Wenger et al. 2011; Isaak, Wenger et al. 2017). For each transect in the riparian inventory, we appended values from three predicted scenarios from the closest NorWeST model data location. The modeled scenarios were a 'current condition' composite average MWMT between 1993 and 2011 (hereafter referred to as 2002, the midpoint of the modeled years), the predicted MWMT for 2040, and the predicted MWMT for 2080 (the 2040 and 2080 scenarios include the effect of lower climate change increases in smaller, colder streams (Luce, Staab et al. 2014). We next calculated the yearly water temperature change between 2002 and 2040, and the yearly change between 2040 and 2080 at each riparian inventory location.

We modeled water temperature into the future in one year increments. At each time step, we calculated tree height (current height plus modeled annual growth) and canopy opening angle, and then computed pre-climate change water temperature using the empirical stream temperature equation. We then added the climate change increase for that time step to compute future stream temperature. If the time step was before 2040 we added the yearly climate change increase for 2002-2040; if the time step was after 2040, we added the 2040-2080 climate change increase. To visualize the effect of tree growth on future water temperature using our model, we present the results of the climate change contribution to water temperature alone and in combination with the tree growth model.

Juvenile salmonid growth is diminished or eliminated when water temperature exceeds ~19.1 ˚C (the sub-lethal growth stress limit for juvenile Chinook, defined as 20 % lower growth than under optimal conditions; Armour 1991; McCullough, Spalding et al. 2001), and the upper lethal threshold for juvenile salmonids is ~23 ˚C (Brett 1952). To assess the length of river predicted to exceed these temperature thresholds, we appended mean modeled temperatures (current, historical, and future 2040 and 2080) from within a 50 m search radius to each reach within the National Hydrography Dataset for reaches covered by the riparian inventory. We then calculated the total length of stream exceeding each temperature threshold for each time period.

Additionally, we examined patterns of stream temperature with respect to channel width in the current and future scenarios. Because stream temperature varies widely at any given channel width, we lumped the temperature data into 10 channel width bins. Because there are many more transect locations in narrow channels than wider channels, we chose to enforce equal numbers of transects within each bin while allowing the channel width range encompassed by each bin to vary.

Results

Remote measurement of canopy opening angle

Current canopy opening angles ranged between 0˚ (canopy completely closed) and 180˚ (both banks bare) in the portions of the Chehalis River basin covered by the lidar topographic datasets (Fig. 3A). Historical canopy opening angles ranged from 0˚ to 145˚ (Fig. 3B), and change in canopy opening angle ranged from -19.4˚ to 180˚ (Fig. 3C). The negative numbers represent sites expected to have deciduous species based on bankfull width but which in reality have taller-than-expected deciduous or conifer trees (~1.2 % of all sites). For transects with a tree height greater than zero, canopy opening angle change was greatest at channel widths between ~5 m and ~40 m (Fig. 3D). The exact location of the maximum was dependent on current tree height. For canopy opening widths larger than ~100 m, canopy angle change was always less than 50˚. Spatially, developed and agricultural areas in the south-eastern portion of the basin exhibited the highest values of canopy opening angle change; the mainstem Chehalis River has experienced intermediate canopy angle change; and upland forested tributaries have experienced the least change, at least in regions for which we have lidar data.

Figure 3.

Modeling stream water temperature

We accepted the mean value of each model coefficient from the cross validation tests (Fig. 4A) to construct the Chehalis Stream Temperature Model (CSTM) based on several pieces of evidence. First, histograms of the coefficients from each test were approximately normally distributed (not shown), suggesting that the mean coefficient best represented the central tendency. Second, the adjusted R^2 values fell in a narrow range between 0.59 and 0.62, with one exception (when data for the year 2010 were removed the adjusted R^2 was 0.70 due to the removal of one outlier). Third, the maximum range in modeled temperatures across all cross validation tests was limited to +/- 0.98 ˚C at high canopy opening angles and low drainage areas (Fig. 4B); the minimum range (+/- 0.13 ˚C) occurs in the diagonal of the parameter space where the data are concentrated. The final model was

$$T = -9.15 + 0.035\theta_{c,H} + 3.00\log(A) \quad (2)$$

where T is water temperature, $\theta_{C,H}$ is canopy opening angle, and A is drainage area. For the 11 NorWeST sites, the maximum modeled water temperature was 23.4 ˚C and the minimum temperature was 13.4 ˚C (Fig. 4C). The mean adjusted R^2 from the cross validation tests was 0.61 (when we ran the same cross-validation test using drainage area as the lone predictor, the mean adjusted R^2 was 0.59). The mean model predicted the measured temperatures with an R^2 of 0.63 (Fig. 4D). The root mean squared error was 2.29 ˚C.

Figure 4.

When the final model was applied to the riparian dataset, modeled August MWMT in the Chehalis Basin ranged up to 26.2 ˚C under current conditions, with 53.2 km of river exceeding 23 ˚C (Fig. 5A). Approximately 254 river kilometers exceeded 19.1 ˚C. Historical modeled temperatures ranged up to 24.9 ˚C, with 167.1 km exceeding 19.1 ˚C (~52 % increase in the current condition) and only 15.8 km exceeding 23 ˚C (~237 % increase in the current condition; Fig. 5B). Temperature change ranged between -0.68 ˚C and 6.32 ˚C, with the highest levels of change concentrated in the urban and agricultural southeast part of the basin (Fig. S3).

Figure 5.

Table 1.

Future stream temperature: tree growth and climate change

The CSTM predicted increases in temperature due to climate change and a cooling effect in many reaches due to tree growth (table 1). The model predicted an increase to the maximum basin-wide MWMT due to climate change alone of 1.8 ˚C by 2040 and 3.0 ˚C by 2080 (these numbers follow directly from the NorWeST prediction). When tree growth was included, the predicted increase to the maximum temperature above current conditions was 0.6 ˚C in 2040 and 1.7 ˚C in 2080 (roughly 50-67 % less than the predicted increase without tree growth). By 2040, the length of river predicted to exceed 19.1 ˚C was 528.9 km in the climate change-only model (108 % increase over current conditions) and 398.7 km when tree growth was included (57 % increase over current conditions). For the same time period, the length of river predicted to exceed 23 ˚C was 129.6 km in the climate change-only model (144 % increase above current conditions) and 96.2 when tree growth was included (81 % increase above current conditions). By 2080, the climate change-only model predicted that 693.4 km will exceed 19.1 ˚C (173 % increase above current conditions); 536.6 km was predicted to exceed 19.1 ˚C when tree growth was included (111 % increase above current). The length of river predicted to exceed 23 ˚C by 2080 in the climate change-only model was 204.5 km (284 % increase above current conditions) and 141.5 km when tree growth was included (167 % increase above current conditions).

Maximum stream temperature within channel width bins increased with increasing channel width, consistent with the hypothesis (Fig. 6A). At channel widths greater than ~90 m, maximum temperatures did not change between 2002 and 2020 but then rose steadily between 2020 and 2080 (Fig. 6A). For channel widths less than ~90 m, stream temperatures decreased dramatically in the first 20 years of the simulation followed by a gradual increase through 2080. For channel widths less than ~50 m, the final 2080 maximum temperature was equivalent to or less than the current temperature (Fig. 6A). In contrast, when tree growth was neglected from the model temperatures steadily rose throughout the simulation (Fig. 6B).

Figure 6.

Discussion

Our results indicate that canopy opening angle and drainage area alone explain up to ~63 % of the variation in measured water temperatures in the Chehalis River basin (Fig. 4D). Combined with our canopy opening analysis, the CSTM illustrates the spatial distribution of riparian degradation and temperature change (Figs. 3C, S3), with lowland urban and agricultural areas experiencing the highest level of change and forested areas experiencing lower levels of change relative to historical conditions.

Stream temperature models may be broadly classified into empirical and process-based (physical) models. Process-based models use physical principles to track heat input, output and movement within a reach of study (Brown 1972; Beschta and Weatherred 1984; Boyd and Kasper 2003; Caissie, Satish et al. 2007). Such models can provide highly accurate predictions of stream temperature but they generally require detailed calibration data relating to channel geometry, basin hydrology, climatology, and meteorology that may be difficult to apply or even collect over large river basins or throughout regions (Benyahya, Caissie et al. 2007). In contrast, empirical (statistical) models predict stream temperature from basin, land use and climatological variables that may be readily available as GIS datasets (Isaak, Wenger et al. 2011; Hill, Hawkins et al. 2013; Hill, Hawkins et al. 2014). These models commonly rely on point measurements of temperature made throughout many river basins, and have been shown to reliably and accurately reproduce river water temperatures at a range of scales using conventional and more complex spatial statistical methods (e.g.Ahmadi-Nedushan, St-Hilaire et al. 2007; Benyahya, Caissie et al. 2007; Isaak, Wenger et al. 2011; Hill, Hawkins et al. 2013; Hill, Hawkins et al. 2014; Isaak, Peterson et al. 2014).

The CSTM compliments previous stream temperature modeling efforts by employing airborne lidar data to measure riparian condition at very high resolution. To assess the CSTM output in relation to another regional stream temperature model, we compared our results to the NorWeST predictive model for western Washington (Isaak, Wenger et al. 2011). In its calibration, the NorWeST predictive model uses data from hundreds of sites distributed throughout western Washington, including the same sites we used to train our model. The composite historical MWMT scenario for 1993-2011 (the same scenario we used as our baseline 'current condition' to calculate the climate change increases) comprises a similar range of years as the data available for the Chehalis River basin. We appended the NorWeST predictions to our riparian dataset locations using a spatial join in ArcGIS, and plotted the stream temperature difference (NorWeST temperature minus CSTM temperature) against channel width (Fig. 7A). At small channel widths, the NorWeST temperatures are on average 7.9 ˚C warmer than the CSTM predicts. The difference decays with increasing channel width (as riparian condition becomes less and less important); however, the mean difference does not decrease below 0.6 ˚C throughout the dataset. We also plotted the residual between the NorWeST raw data and the NorWeST predictive model and the CSTM (data minus model for each; Fig. 7B). We found that the NorWeST prediction overestimates temperatures at narrow channel widths (up to ~45 m) in the Chehalis River basin. In contrast, the CSTM is better distributed about the zero line at small to intermediate channel widths (i.e. is more accurate in that range). This may reflect better model performance when riparian shade is quantified with high resolution, or simply that the NorWeST model is less accurate in small streams of the

Chehalis basin because it was constructed with a broad regional dataset that includes rivers from Puget Sound and the Olympic Peninsula. Regression of predicted vs observed temperature for the NorWeST Washington Coast model domain (https://www.fs.fed.us/rm/boise/AWAE/projects/NorWeST/ModeledStreamTemperatureScenarioMaps.shtml) showed that the NorWeST model tended to slightly over-predict temperature when observed temperatures were low (intercept above zero), but overall the NorWeST model was very accurate and precise for the region. Notably, the CSTM predictions deviate from the regional NorWeST model in exactly the portion of the network expected to be most affected by riparian shade.

Errors in water temperature models in small- to intermediate-sized channels that are based on regional calibration are consistent with a growing body of literature demonstrating complex patterns of stream temperature in small, cool mountain streams (Arismendi, Johnson et al. 2012; Luce, Staab et al. 2014; Lisi, Schindler et al. 2015; Isaak, Young et al. 2016). Air temperature, which drives much of the spatial variability in the NorWeST model, has been shown to be at least partially decoupled from stream temperature in the highest and coldest mountain streams (Luce, Staab et al. 2014; Lisi, Schindler et al. 2015). While previous work has attributed the lower sensitivity between stream and air temperature in small, cool streams to snowmelt and geomorphological effects, few streams in the Chehalis River basin are fed by snowmelt in August, suggesting this is not a significant source of the mismatch between air and stream temperatures in our study basin. Instead, our results are consistent with riparian vegetation also playing a role in some streams by providing shade and creating an insulated microclimate along the river corridor (Luce, Staab et al. 2014). The NorWeST model quantifies riparian condition using 30 m resolution canopy data, which is surely appropriate for larger rivers but may miss important details in channels that are narrower than 30 m. Therefore, it is possible that riparian vegetation can explain at least some of the residual between the NorWeST prediction and the data in small- to intermediate-sized channels.

Figure 7.

We attribute the error in the CSTM (RMSE = 2.29 ˚C) to sources of temperature variability not captured by our analysis, such as hyporheic exchange, as well as to between-year variability. Additionally, our method does not account for tributary inputs, which may be better treated by process-based models or spatial-statistical models. Moreover, our method does not account for the width of the riparian forest, which plays a significant role in mitigating light flux to streams (Kiffney, Richardson et al. 2003). In much of the Chehalis River basin, buffers at least 30 m wide have been left on active forest harvest lands. In other regions, such as near agricultural and urban areas, the riparian forest has been completely removed. While our model accounts for the greatest proportion of change in solar radiation reaching the stream by incorporating canopy opening angle, it may overestimate the influence of riparian shade in reaches where narrow buffers remain.

Additionally, removal of riparian vegetation may destabilize channel banks, leading to channel widening due to geomorphic processes (White, Justice et al. 2017). In reaches where channel widening has occurred, our assumption of no widening will lead us to over-predict canopy opening angle change. White et al. (2017) applied a channel narrowing restoration scenario to two degraded tributaries of the Columbia River, and found water temperature reductions of 2.2 ˚C and 0.6 ˚C in each tributary, respectively, resulting from restoration of historical channel width alone (i.e. without increased shade from revegetation). While insightful, the analysis relied on extensive and time-consuming mapping of historical channel conditions using notes from the General Land Office. Our method, in contrast, may miss the effect of channel widening due to land use change, yet benefits from rapid deployment over large regions of lidar coverage.

Despite the above caveats, the range in modeled temperature change we observed overlaps with the range from a meta-analysis (Moore, Spittlehouse et al. 2005), lending confidence to our model predictions. However, we caution that despite the high resolution of the riparian dataset (10 m spaced transects), accuracy of the temperature model at any one site is limited by omission of variables for which we have no data. Moreover, the small sample size of unique NorWeST training data locations reduces confidence in the model, particularly extrapolating to sub-basins not represented in the NorWeST temperature database. As a result of the complex dynamics influencing local temperatures, and the limited number of Chehalis basin sites the NorWeST dataset, site specific estimates of water temperature are likely to be somewhat uncertain. However, we expect errors in the temperature model to be consistent between scenarios, making comparisons between current, historical, and future conditions more reliable even where absolute temperatures are less accurate.

Channel width in both alluvial and bedrock channels commonly increases in the downstream direction to maintain the balance between transport capacity of the river with sediment supply (Leopold and Maddock 1953; Hack 1957; Montgomery and Gran 2001; Finnegan, Roe et al. 2005). Despite local variations due to land use changes or lithologic contacts (Montgomery and Gran 2001), it is this physical reality in most drainage basins that leads to one of the main effects we have documented in this study: expected riparian shade under natural conditions is inversely related to drainage area and channel width. Further, as we have hypothesized based on the geometry of the canopy opening angle, change in shade after disturbance is also a function of channel width. These results may help guide limited restoration dollars to the areas of river basins that are most in need of restoration, and that have the highest potential for reducing summer stream temperatures in the future.

Conclusion

Based on the simple geometrical relationship formed by the channel width and current, historical and future tree heights, we have shown that riparian shade reduction or increase is a function of channel width as well as tree height. Because stream temperature is correlated with the canopy opening angle, temperature change due to shade reduction varies depending on position within the river basin as a function of downstream changes in hydraulic geometry. Moreover, because riparian restoration may be more effective for managing and restoring stream temperatures at small to intermediate channel widths, the CSTM predicts similar maximum temperatures in 2080 as the current condition in the upper portions of the river network whereas overall maximum temperatures may rise by as much as 3.0 ˚C. River restoration is a multi-million dollar endeavor (e.g. Malakoff 2004), and managers commonly desire quantitative criteria by which to guide restoration money and effort. Our results suggest that a physical and riparian forest context of river basins may be used to guide restoration of riparian shade to maximum effect. Because restoration efforts should be executed with the goal of enhancing natural processes, not fighting them (Beechie, Sear et al. 2010), it is vital that potential for restoration due to channel width *and* tree height be considered when planning riparian interventions.

Supporting Information

Additional supporting information may be found online under the Supporting Information tab for this article: Figures which provide additional context for our riparian prediction, historical reference condition analysis, and temperature modeling results.

Data Availability

All lidar DEM products are publically available after registration from the Puget Sound lidar Consortium (pugetsoundlidar.ess.washington.edu). The Matlab codes used to generate the riparian dataset are available at https://github.com/gseixas/Seixas-et-al-Influence-of-channel-width-on-stream-shade-and-temperature-change, or from the authors. Three-dimensional animated versions of figure 4A-C are also available at the github repository. GIS data are available from the authors upon request.

Acknowledgments

This work was supported by the Washington State Department of Fish and Wildlife as part of a broader effort to understand restoration possibilities in the Chehalis River basin. We would like to thank Drs. Martin Liermann, John Quinn, and George Pess for thoughtful comments on an early draft of the manuscript. Two anonymous reviewers greatly helped refine the clarity and scope of the final manuscript.

Literature Cited

Agee, J. K., 1988. Successional dynamics in forest riparian zones. *In*: *Streamside Management: Riparian Wild Life and Forestry Interactions,* K. J. Raedeke (K. J. Raedeke)K. J. Raedekes). University of Washington Press, Seattle, WA, pp. 31-43.

Agee, J. K., 1993. *Fire ecology of Pacific Northwest forests*. Washington, D.C., Island press, ISBN 1610913787

Ahmadi-Nedushan, B., A. St-Hilaire, T. B. Ouarda, L. Bilodeau, E. Robichaud, N. Thiemonge and B. Bobee, 2007. Predicting river water temperatures using stochastic models: case study of the Moisie River (Québec, Canada). *Hydrological Processes* **21**:21-34. https://doi.org/10.002/hyp.6353.

Allen, D., W. Dietrich, P. Baker, F. Ligon and B. Orr, 2007. Development of a mechanistically based, basin-scale stream temperature model: applications to cumulative effects modeling.

Arismendi, I., S. L. Johnson, J. B. Dunham, R. Haggerty and D. Hockman-Wert, 2012. The paradox of cooling streams in a warming world: regional climate trends do not parallel variable local trends in stream temperature in the Pacific continental United States. *Geophysical Research Letters* **39**. https://doi.org/10.1029/2012GL051448.

Armour, C., 1991. Guidance for evaluating and recommending temperature regimes to protect fish. *In: Instream flow information paper 28,* U.S. Department of the Interior, Fish and Wildlife Service, Biological Report 90(22).

Beechie, T. J., M. Liermann, M. M. Pollock, S. Baker and J. Davies, 2006. Channel pattern and river-floodplain dynamics in forested mountain river systems. *Geomorphology* **78**:124-141. https://doi.org/10.1016/j.geomorph.2006.01.030.

Beechie, T. J., G. Pess, P. Kennard, R. E. Bilby and S. Bolton, 2000. Modeling recovery rates and pathways for woody debris recruitment in northwestern Washington streams. *North American Journal of Fisheries Management* **20**:436-452. https://doi.org/10.1577/1548-8675(2000)020<0436:MRRAPF>2.3.CO;2.

Beechie, T. J., D. A. Sear, J. D. Olden, G. R. Pess, J. M. Buffington, H. Moir, P. Roni and M. M. Pollock, 2010. Process-based principles for restoring river ecosystems. *BioScience* **60**:209-222. https://doi.org/10.1525/bio.2010.60.3.7.

Benyahya, L., D. Caissie, A. St-Hilaire, T. B. Ouarda and B. Bobée, 2007. A review of statistical water temperature models. *Canadian Water Resources Journal* **32**:179-192. https://doi.org/10.4296/cwrj3203179.

Beschta, R., R. Bilby, G. Brown, L. Holtby and T. Hofstra, 1987. Stream Temperature and Aquatic Habitat: Fisheries and Forestry Implications. *Streamside Management: Forestry and Fisheries Interactions*.

Beschta, R. L., 1997. Riparian shade and stream temperature: an alternative perspective. *Rangelands*:25-28.

Beschta, R. L. and J. D. Weatherred, 1984. *TEMP-84: a computer model for predicting stream temperatures resulting from the management of streamside vegetation*, US Forest Service, Watershed Systems Development Group,

Boyd, M. and B. Kasper, 2003. Analytical methods for dynamic open channel heat and mass transfer: Methodology for heat source model Version 7.0. *Watershed Sciences Inc., Portland, Oregon, USA*.

Bresenham, J. E., 1965. Algorithm for computer control of a digital plotter. *IBM Systems journal* **4**:25-30.

Brett, J. R., 1952. Temperature tolerance in young Pacific salmon, genus Oncorhynchus. *Journal of the Fisheries Board of Canada* **9**:265-323.

Brosofske, K. D., J. Q. Chen, R. J. Naiman and J. F. Franklin, 1997. Harvesting effects on microclimatic gradients from small streams to uplands in western Washington. *Ecol Appl* **7**:1188-1200. https://doi.org/10.1890/1051-0761(1997)007[1188:HEOMGF]2.0.CO;2.

Brown, G., 1972. An improved temperature model for small streams. *Water Resources Research Institute Report* **16**.

Brown, G. W. and J. T. Krygier, 1970. Effects of Clear-Cutting on Stream Temperature. *Water Resources Research* **6**:1133-1139. https://doi.org/10.1029/WR006i004p01133.

Caissie, D., 2006. The thermal regime of rivers: a review. *Freshwater Biology* **51**:1389-1406. https://doi.org/10.1111/j.1365-2427.2006.01597.x.

Caissie, D., M. G. Satish and N. El-Jabi, 2007. Predicting water temperatures using a deterministic model: Application on Miramichi River catchments (New Brunswick, Canada). *Journal of Hydrology* **336**:303-315. https://doi.org/10.1016/j.jhydrol.2007.01.008.

Chen, Y. D., R. F. Carsel, S. C. McCutcheon and W. L. Nutter, 1998. Stream temperature simulation of forested riparian areas: I. Watershed-scale model development. *Journal of Environmental Engineering* **124**:304-315.

Prism Climate Group, 2012. 30 year normals, Oregon State University. *http://prism.oregonstate.edu.*

Crocker, R. L. and J. Major, 1955. Soil development in relation to vegetation and surface age at Glacier Bay, Alaska. *The Journal of Ecology*:427-448. https://doi.org/10.2307/2257005.

Davies-Colley, R. J. and J. M. Quinn, 1998. Stream lighting in five regions of North Island, New Zealand: Control by channel size and riparian vegetation. *New Zealand Journal of Marine and Freshwater Research* **32**:591-605. https://doi.org/10.1080/00288330.1998.9516847.

Davies, J. R., K. M. Lagueux, B. Sanderson and T. J. Beechie, 2007. Modeling Stream Channel Characteristics From Drainage-Enforced DEMs in Puget Sound, Washington, USA1. *JAWRA Journal of the American Water Resources Association* **43**:414-426. https://doi.org/10.1111/j.1752-1688.2007.00032.x.

Farr, W. A., 1984. Site index and height growth curves for unmanaged even-aged stands of western hemlock and Sitka spruce in southeast Alaska, *United States Department of Agriculture, Forest Service Research Paper, PNW-326.*

Finnegan, N. J., G. Roe, D. R. Montgomery and B. Hallet, 2005. Controls on the channel width of rivers: Implications for modeling fluvial incision of bedrock. Geology 33:229-232. https://doi.org/10.1130/G21171.1.

Fonda, R., 1974. Forest succession in relation to river terrace development in Olympic National Park, Washington. *Ecology* **55**:927-942. https://doi.org/10.2307/1940346.

Franklin, J. F. and C. T. Dyrness, 1973. Natural vegetation of Oregon and Washington, *United States Department of Agriculture, Pacific Northwest Forest and Range Experiment Station, General Technical Report PNW-8.*

Fullerton, A. H., C. E. Torgersen, J. J. Lawler, R. N. Faux, E. A. Steel, T. J. Beechie, J. L. Ebersole and S. G. Leibowitz, 2015. Rethinking the longitudinal stream temperature paradigm: region-wide comparison of thermal infrared imagery reveals unexpected complexity of river temperatures. *Hydrological Processes* **29**:4719-4737. https://doi.org/10.1002/hyp.10506.

Gannett, H., 1899. The forests of the United States, *Department of the Interior, United States Geological Survey.*

Hack, J. T., 1957. Studies of longitudinal stream profiles in Virginia and Maryland, *United States Geological Survey Professional Paper 294-B:45-97.*

Harrington, C. A. and R. O. Curtis, 1986. Height growth and site index curves for red alder. *United States Department of Agriculture Pacific Northwest Research Station, Research Paper PNW-358.*

Hicks, B. J., J. D. Hall, P. Bisson and J. R. Sedell, 1991. Responses of salmonids to habitat changes, *In* Meehan, W.R. *ed.,* Influences of Forest and Rangeland Management on Salmonid Fishes and Their Habitats, *American Fisheries Society Special Publication 19:483-518.*

Hill, R. A., C. P. Hawkins and D. M. Carlisle, 2013. Predicting thermal reference conditions for USA streams and rivers. *Freshwater Science* **32**:39-55. https://doi.org/10.1899/12-009.1.

Hill, R. A., C. P. Hawkins and J. Jin, 2014. Predicting thermal vulnerability of stream and river ecosystems to climate change. *Climatic change* **125**:399-412. https://doi.org/10.1007/s10584-014-1174-4.

Isaak, D., S. Wenger, E. Peterson, J. Ver Hoef, S. Hostetler, C. Luce, J. Dunham, J. Kershner, B. Roper and D. Nagel, 2011. NorWeST: an interagency stream temperature database and model for the Northwest United States. *US Fish and Wildlife Service, Great Northern Landscape Conservation Cooperative Grant. Project website: www. fs. fed. us/rm/boise/AWAE/projects/NorWeST. html*.

Isaak, D., S. Wollrab, D. Horan and G. Chandler, 2012. Climate change effects on stream and river temperatures across the northwest US from 1980–2009 and implications for salmonid fishes. *Climatic Change* **113**:499-524. https://doi.org/10.1007/s10584-011-0326-z.

Isaak, D., M. Young, C. Luce, S. Hostetler, S. Wenger, E. Peterson, J. Ver Hoef, M. Groce, D. Horan and D. Nagel, 2016. Slow climate velocities of mountain streams portend their role as refugia for cold-water biodiversity. *Proceedings of the National Academy of Sciences of the United States of America* **113**:4374-4379. https://doi.org/10.1073/pnas.1522429113.

Isaak, D. J., E. E. Peterson, J. M. Ver Hoef, S. J. Wenger, J. A. Falke, C. E. Torgersen, C. Sowder, E. A. Steel, M.-J. Fortin, C. E. Jordan, A. S. Ruesch, N. Som and P. Monestiez, 2014. Applications of spatial statistical network models to stream data. *Wiley Interdisciplinary Reviews: Water* **1**:277-294. doi: 10.1002/wat2.1023.

Isaak, D. J., S. J. Wenger, E. E. Peterson, J. M. Ver Hoef, D. E. Nagel, C. H. Luce, S. W. Hostetler, J. B. Dunham, B. B. Roper and S. P. Wollrab, 2017. The NorWeST Summer Stream Temperature Model and Scenarios for the Western US: A Crowd-Sourced Database and New Geospatial Tools Foster a User Community and Predict Broad Climate Warming of Rivers and Streams. *Water Resources Research*. https://doi.org/10.1002/2017WR020969.

Kaylor, M. J., D. R. Warren and P. M. Kiffney, 2017. Long-term effects of riparian forest harvest on light in Pacific Northwest (USA) streams. *Freshwater Science* **36**:000-000. https://doi.org/10.1086/690624.

Kiffney, P. M., C. M. Greene, J. Hall and J. Davies, 2006. Tributary streams create spatial discontinuities in habitat, biological productivity, and diversity in mainstem rivers. *Canadian Journal of Fisheries and Aquatic Sciences* **63**:2518-2530. https://doi.org/10.1139/f06-138.

Kiffney, P. M., J. S. Richardson and J. P. Bull, 2003. Responses of periphyton and insects to experimental manipulation of riparian buffer width along forest streams. *J Appl Ecol* **40**:1060-1076. https://doi.org/10.1111/j.1365-2664.2003.00855.x.

Leopold, L. B. and T. Maddock, 1953. The hydraulic geometry of stream channels and some physiographic implications. *United States Geological Survey Professional Paper 252*.

Leopold, L. B., M. G. Wolman and J. P. Miller, 1964. *Fluvial processes in geomorphology*. New York, Dover Publications, Inc., ISBN 0486139735.

Lisi, P. J., D. Schindler, T. Cline, M. Scheuerell and P. B. Walsh, 2015. Watershed geomorphology and snowmelt control stream thermal sensitivity to air temperature. *Geophysical Research Letters* **42**:3380-3388. https://doi.org/10.1002/2015GL064083.

Luce, C., B. Staab, M. Kramer, S. Wenger, D. Isaak and C. McConnell, 2014. Sensitivity of summer stream temperatures to climate variability in the Pacific Northwest. *Water Resources Research* **50**:3428-3443. https://doi.org/10.1002/2013WR014329.

Macfarlane, W. W., J. T. Gilbert, M. L. Jensen, J. D. Gilbert, N. Hough-Snee, P. A. McHugh, J. M. Wheaton and S. N. Bennett, 2016. Riparian vegetation as an indicator of riparian condition: Detecting departures from historic condition across the North American West. *Journal of environmental management 202(2):447-460.* https://doi.org/10.1016/j.jenvman.2016.10.054.

Malakoff, D., 2004. The river doctor. *Science* **305**:937.

McArdle, R. E., W. H. Meyer and D. Bruce, 1930. The yield of Douglas-fir in the Pacific Northwest. *US Dept. Agr. Tech. Bul* **201**:G4.

McCullough, D., S. Spalding, D. Sturdevant and M. Hicks, 2001. Summary of technical literature examining the physiological effects of temperature on salmonids. *US Environmental Protection Agency Report USEPA-910-D-01-005* **Issue paper 5**.

Means, J. E., S. A. Acker, B. J. Fitt, M. Renslow, L. Emerson and C. J. Hendrix, 2000. Predicting forest stand characteristics with airborne scanning lidar. *Photogrammetric Engineering and Remote Sensing* **66**:1367-1372.

Montgomery, D. R. and K. B. Gran, 2001. Downstream variations in the width of bedrock channels. *Water Resources Research* **37**:1841-1846. https://doi.org/10.1029/2000WR900393.

Moore, R., D. Spittlehouse and A. Story, 2005. Riparian microclimate and stream temperature response to forest harvesting: a review. *Journal of the American Water Resources Association* **41**:813-834. https://doi.org/10.1111/j.1752-1688.2005.tb03772.x.

Munger, T. T., 1940. The Cycle from Douglas Fir to Hemlock. *Ecology* **21**:451-459. https://doi.org/10.2307/1930284.

Naiman, R. J., J. S. Bechtold, T. J. Beechie, J. J. Latterell and R. Van Pelt, 2010. A process-based view of floodplain forest patterns in coastal river valleys of the Pacific Northwest. *Ecosystems* **13**:1-31. https://doi.org/10.1007/s10021-009-9298-5.

Poole, G. C. and C. H. Berman, 2001. An Ecological Perspective on In-Stream Temperature: Natural Heat Dynamics and Mechanisms of Human-CausedThermal Degradation. *Environmental Management* **27**:787-802. https://doi.org/10.1007/s002670010188.

Rot, B. W., R. J. Naiman and R. E. Bilby, 2000. Stream channel configuration, landform, and riparian forest structure in the Cascade Mountains, Washington. *Canadian Journal of Fisheries and Aquatic Sciences* **57**:699-707. https://doi.org/10.1139/f00-002.

Rutherford, J. C., S. Blackett, C. Blackett, L. Saito and R. J. Davies-Colley, 1997. Predicting the effects of shade on water temperature in small streams. *New Zealand Journal of Marine and Freshwater Research* **31**:707-721. https://doi.org/10.1080/00288330.1997.9516801.

Sandell, T., J. Fletcher, A. McAninch and M. Wait, 2014. Grays Harbor Juvenile Fish Use Assessment: 2013 Annual Report. Wild Fish Conservancy Northwest, Seattle, WA.

Seavy, N. E., J. H. Viers and J. K. Wood, 2009. Riparian bird response to vegetation structure: a multiscale analysis using lidar measurements of canopy height. *Ecol Appl* **19**:1848-1857. https://doi.org/10.1890/08-1124.1.

Story, A., R. Moore and J. Macdonald, 2003. Stream temperatures in two shaded reaches below cutblocks and logging roads: downstream cooling linked to subsurface hydrology. *Canadian Journal of Forest Research* **33**:1383-1396. https://doi.org/10.1139/x03-087.

Sullivan, K., J. Tooley, K. Doughty, J. E. Caldwell and P. Knudsen, 1990. Evaluation of prediction models and characterization of stream temperature regimes, *Washington Department of Natural Resources Timber/Fish/Wildlife Report TFW-WQ3-90-006.*

Sumioka, S., D. L. Kresch and K. Kasnick, 1998. *Magnitude and frequency of floods in Washington*, *United States Geological Survey Water-Resources Investigations Report 97-4277.*

U.S.G.S, 2013. National Hydrography Geodatabase: The National Map viewer available on the World Wide Web (http://viewer.nationalmap.gov/viewer/nhd.html?p=nhd), Accessed 2016.

Van Pelt, R., T. C. O'Keefe, J. J. Latterell and R. J. Naiman, 2006. Riparian forest stand development along the Queets river in Olympic National Park, Washington. *Ecological Monographs* **76**:277-298. https://doi.org/10.1890/05-0753.

Vannote, R. L., G. W. Minshall, K. W. Cummins, J. R. Sedell and C. E. Cushing, 1980. The river continuum concept. *Canadian journal of fisheries and aquatic sciences* **37**:130-137. https://doi.org/10.1139/f80-017.

White, S., C. Justice, D. Kelsey, D. McCullough and T. Smith, 2017. Legacies of stream channel modification revealed using General Land Office surveys, with implications for water temperature and aquatic life. *Elem. Sci. Anth.* **5**. http://doi.org/10.1525/elementa.192.

Zwieniecki, M. A. and M. Newton, 1999. Influence of streamside cover and stream features on temperature trends in forested streams of western Oregon. *Western Journal of Applied Forestry* **14**:106-113. https://doi.org/10.1093/wjaf/14.2.106.

Tables

Table 1. Temperature modeling results.

Scenario	**Max. MWMT (˚C)**	**River km > 19.1 ˚C (km)**	**River km > 23 ˚C (km)**
Current	26.2	254.0	53.2
Historical	24.9	167.1	15.8
2040 climate change	28.0	528.9	129.6
2040 climate + growth	26.8	398.7	96.2
2080 climate change	29.2	693.4	204.5

2080 climate + growth	27.9	536.6	141.5

Figure captions

Figure 1: Illustration of the canopy opening angle concept. Left column: riparian forest in the historical condition. Right column: riparian forest after clear cut and regrowth (current condition). A) Narrow, low-order channel. θ_H—historical (mature forest) canopy opening angle. θ_C —current canopy opening angle. B) Intermediate width, mid-order channel. Variables in equation 1 shown: H—tree height; W—channel half width; the subscripts 1 and 2 refer to the left and right channel sides, respectively; C) Wide width, high-order channel.

Figure 2. A) Map of the Chehalis River basin including rivers flowing into Grays Harbor. The stream network used in this study is shown in light blue, with the mainstem Chehalis River shown in dark blue. The spatial extents of all publically-available lidar datasets are shown with grey cross-hatching. Red dots show NorWeST temperature data locations. B) lidar difference map (first returns minus ground surface) of a typical stream corridor, overlain by transects calculated by the Matlab algorithm. Black box shows cross section line in C. C) Cross section through the lidar data. θ is schematically drawn.

Figure 3. Patterns of canopy opening angle change in the Chehalis River basin. A) Current canopy opening angle for the regions of the Chehalis River basin covered by lidar datasets. B) Historical canopy opening angle. C) Change in canopy opening angle (calculated by subtracting the data in B from the data in A). D) Canopy opening angle change plotted in the parameter space of figure S1.

Figure 4. Temperature model results. A) Each cross validation test plotted as a surface. Black dots are August MWMT (mean weekly maximum temperature) from the NorWeST database. B) Surface of maximum minus minimum predicted temperature from each cross validation test at each cell in the parameter space. C) Model surface calculated using the mean coefficient from the cross validation tests. D) Measured August MWMT vs. predicted temperature using the model

in C. Three-dimensional animated versions of A, B and C exist in the github repository (see Data Availability statement).

Figure 5. Basin-wide patterns of August MWMT predicted using the model in figure 4C. A) Current temperature. B) Historical temperature. C) Predicted temperature in 2040 with climate change but without tree growth. D) Predicted temperature in 2040 with climate change and tree growth. E) Predicted temperature in 2080 with climate change but without tree growth. F) Predicted temperature in 2080 with climate change and tree growth.

Figure 6. A) Maximum stream temperature within channel width bins as a function of channel width. Snapshots throughout the simulation are shown (2002, 2020, 2040, 2060, and 2080). B) The same as in A but with tree growth neglected from the water temperature model. The locations of the channel width bins are shown as vertical lines.

Figure 7. A) Difference in temperatures predicted by our model and the NorWeST predictive model (NorWeST minus our model) vs. canopy opening width for all riparian inventory locations (grey dots). The mean values within ten bins are shown as a black line. B) Comparison of model residuals (data minus model).

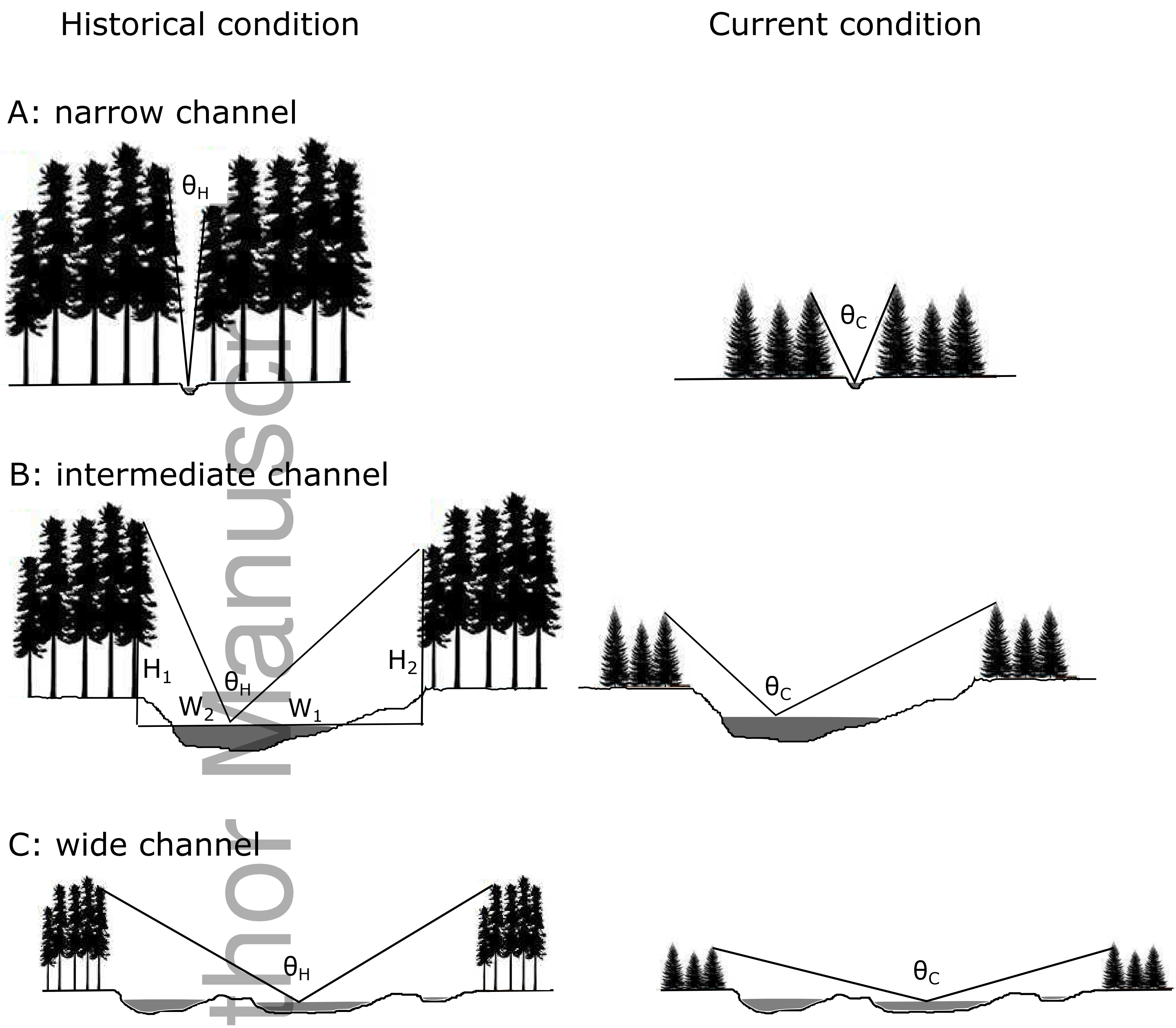

jawra_12655-17-0099_f1.eps

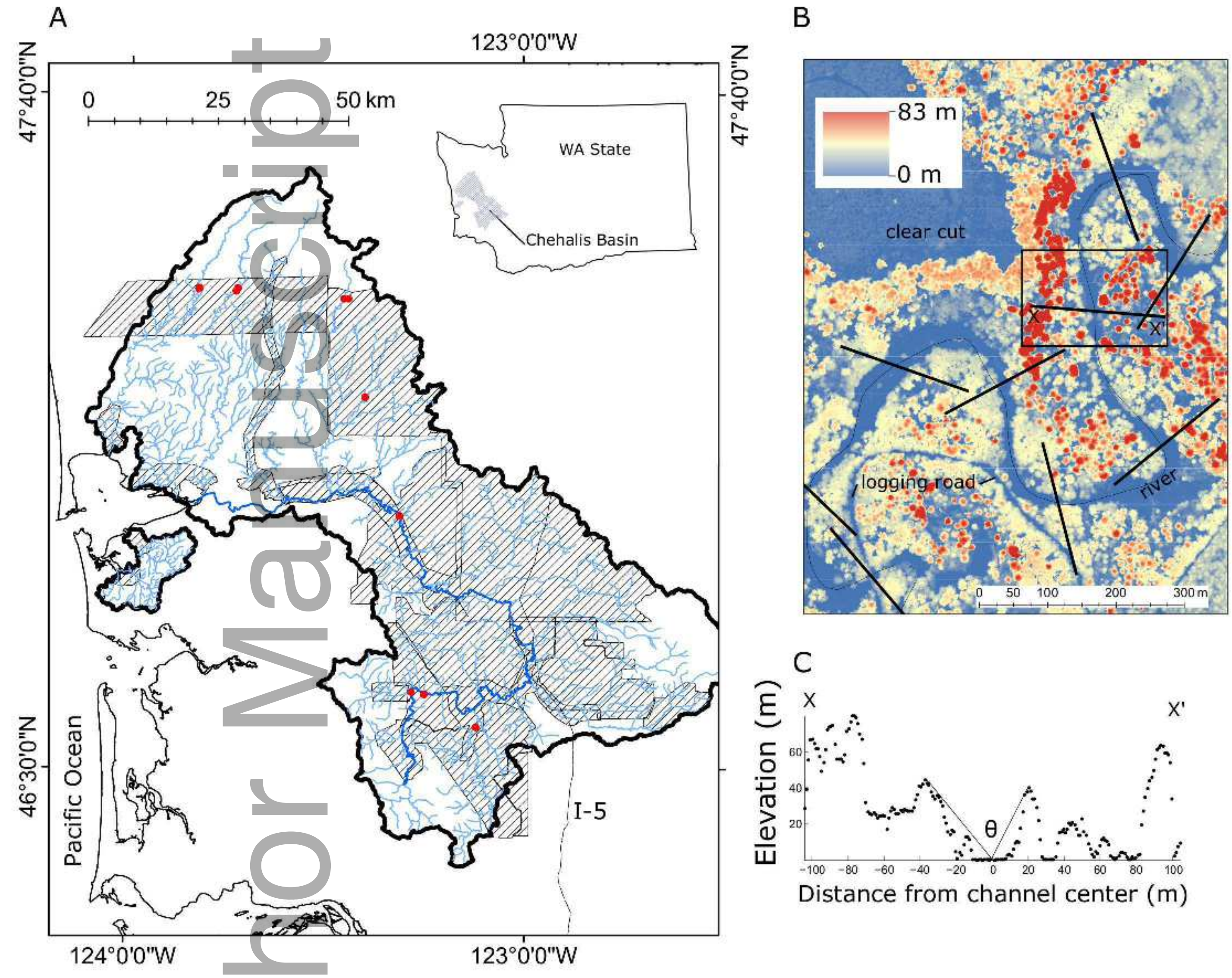
A
123°0'0"W
47°40'0"N
0
25
50 km
WA State
Chehalis Basin
Pacific Ocean
46°30'0"N
I-5
124°0'0"W
B
83 m
0 m
clear cut
logging road
river
X
X'
0
50
100
200
300 m
C
X
X'
Elevation (m)
θ
Distance from channel center (m)

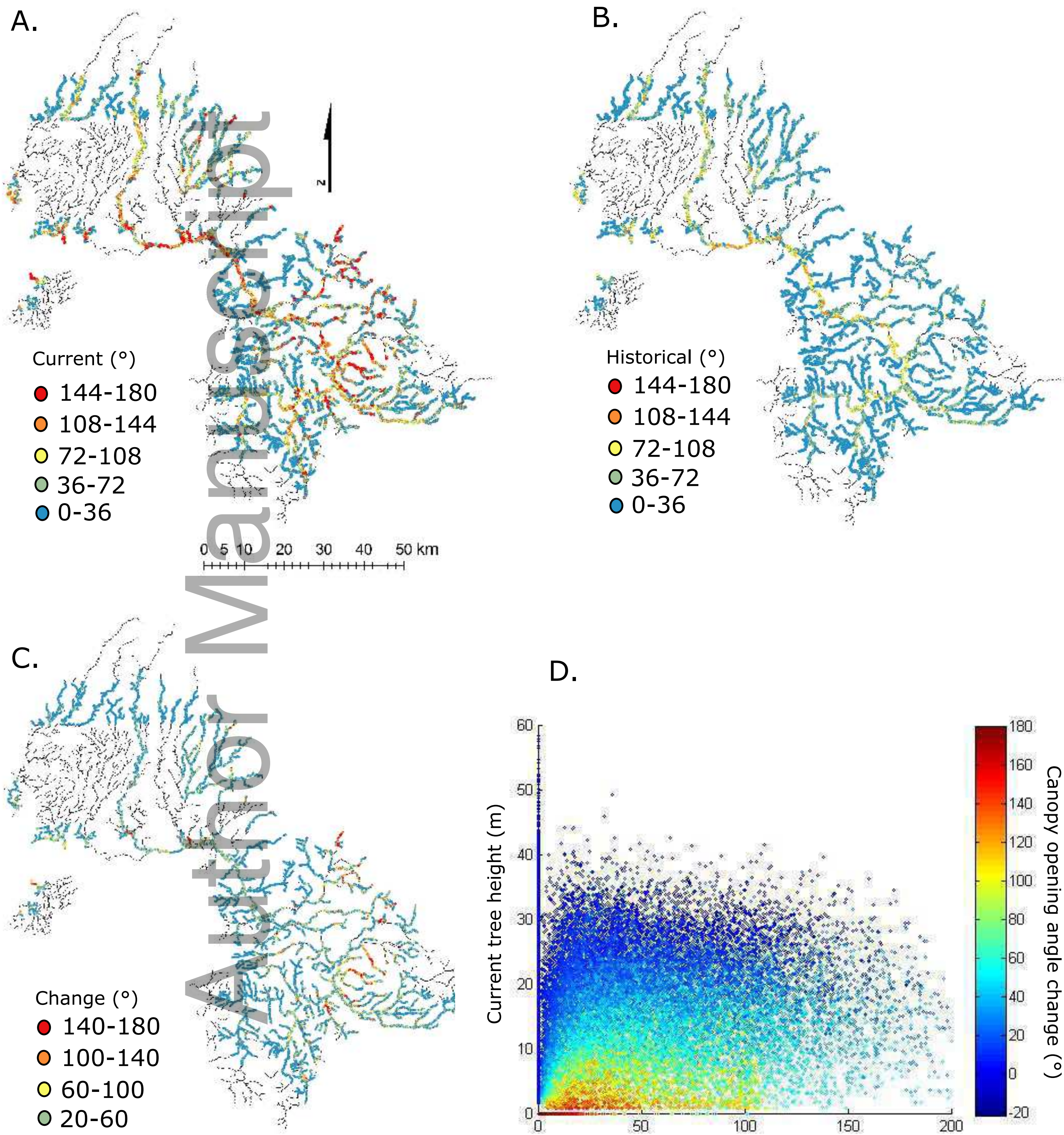

jawra_12655-17-0099_f3.eps

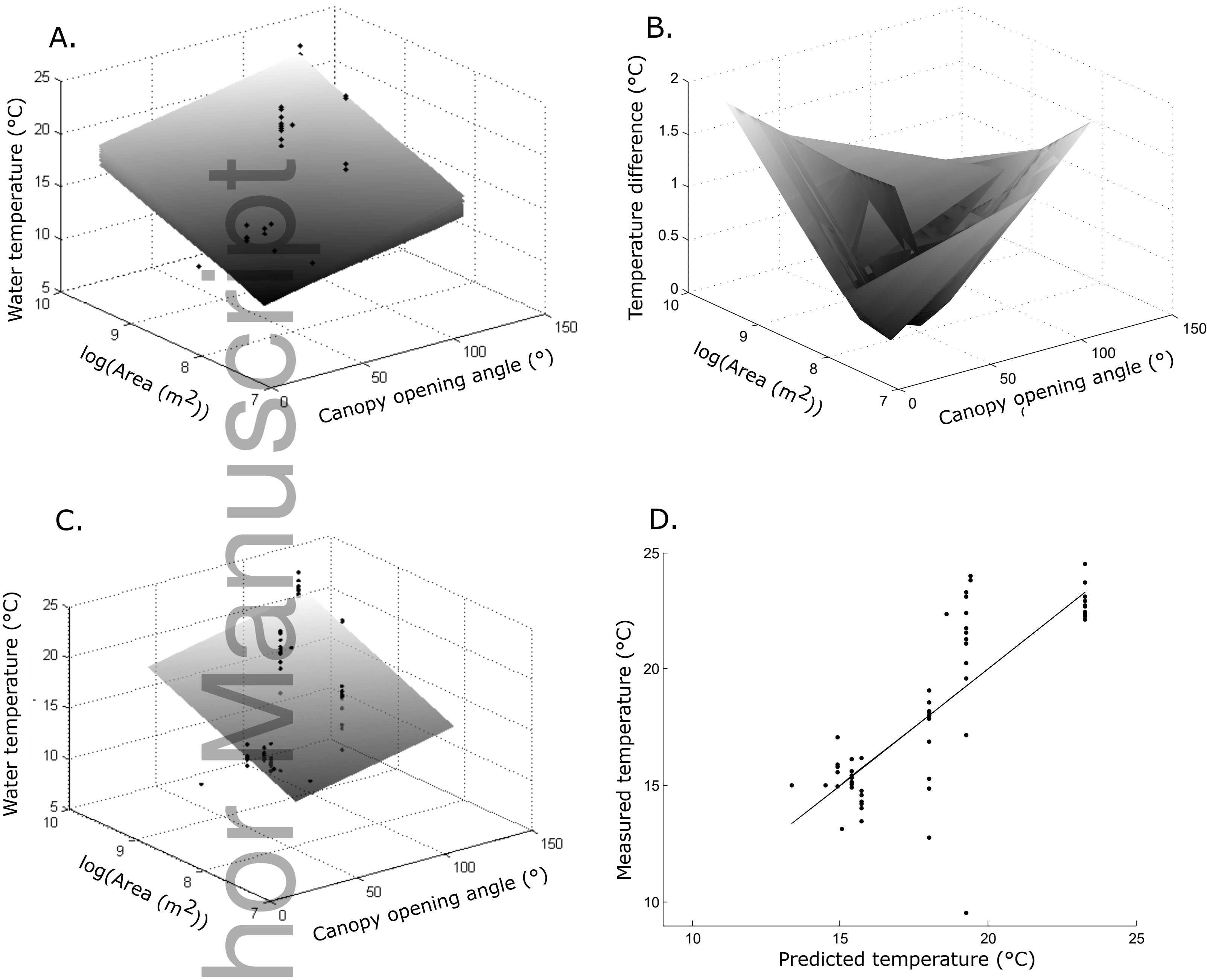

jawra_12655-17-0099_f4.eps

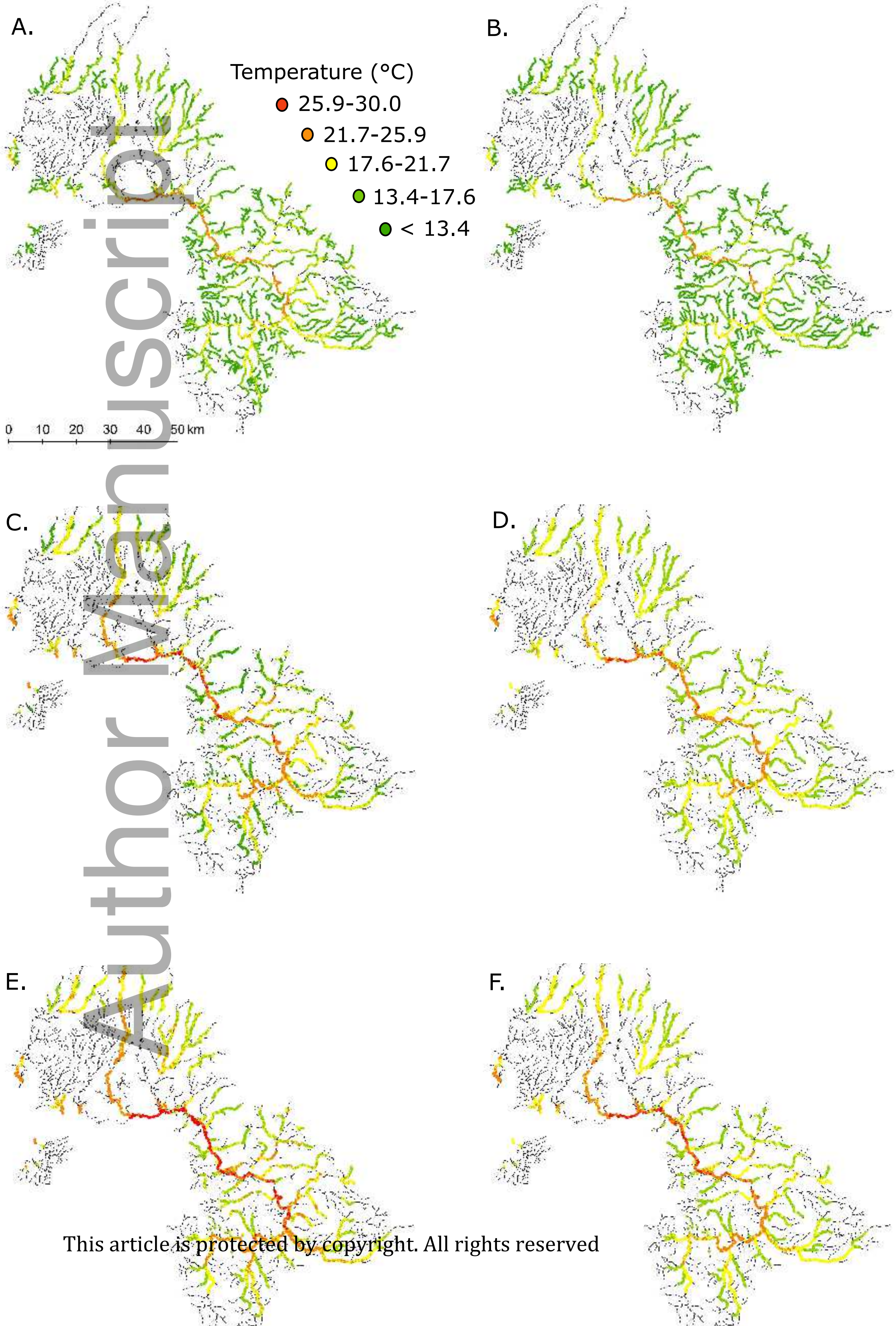
A.
B.
Temperature (°C)
25.9-30.0
21.7-25.9
17.6-21.7
13.4-17.6
< 13.4
0 10 20 30 40 50 km
C.
D.
E.
F.

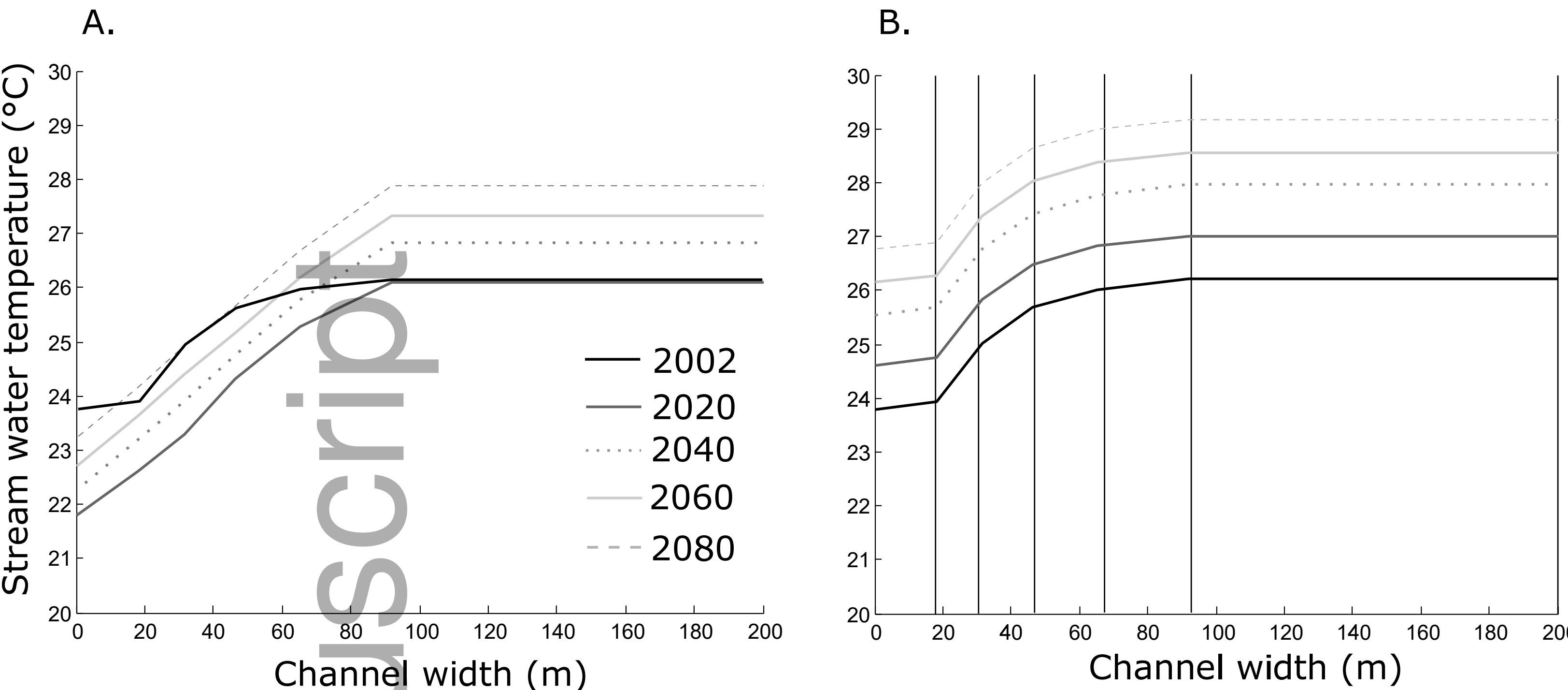

jawra_12655-17-0099_f6.eps

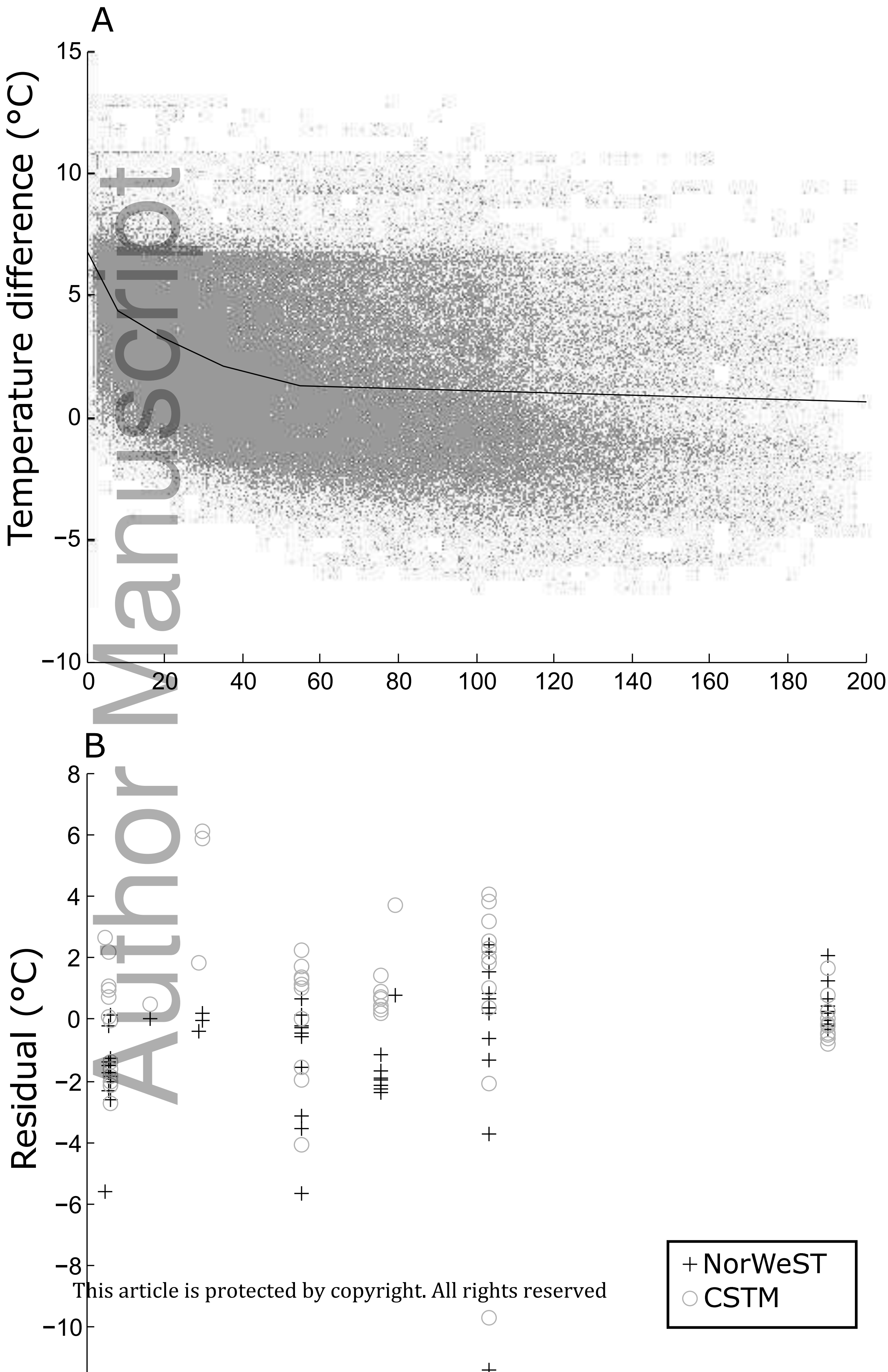
A
Temperature difference (°C)
15
10
5
0
−5
−10
0
20
40
60
80
100
120
140
160
180
200
B
Residual (°C)
8
6
4
2
0
−2
−4
−6
−8
−10
NorWeST
CSTM